

Fig. S1. Procr expression pattern during embryonic development.

(A) Whole-mount in situ hybridization result of *Procr* expression on E8.0 wild-type embryos. Dense positive staining was observed on dorsal aortae, consistent with the staining result from *Procr*^{mGFP-2A-LacZ} reporter embryos. (B) FACS analysis on E8.25 WT embryo endothelium (CD31+) indicate a subpopulation of Procr⁺ ECs. Data in FACS plots are from at least 5 embryos and is presented as mean ± Standard error of the mean (S.E.M). (C-D) Immunohistochemistry of E8.5 *Procr*^{mGFP-2A-LacZ} embryo section indicating the presence of Procr⁺ ECs (indicated as mG⁺) on the forming aorta (out-lined by CD31, white box) and within cardiac cavity (orange box). White boxed area is enlarged at right (D). Procr⁺ cells indicated by yellow arrows. mG, mGFP. (E-F) Immunohistochemistry of E9.5 *Procr*^{mGFP-2A-LacZ} embryo showing Procr⁺ ECs on multiple vascular beds (ERG labels EC nuclei), including the aorta and cardiac cavity (E, yellow arrows) as well as the forming intersomatic vessels and vessel plexus surrounding aorta-gonad-mesonephros (AGM) region (F, yellow arrows). da: dorsal aorta, cc: cardiac cavity, isv: intersomatic vessels. C-F, Scale bars, 50 μm.

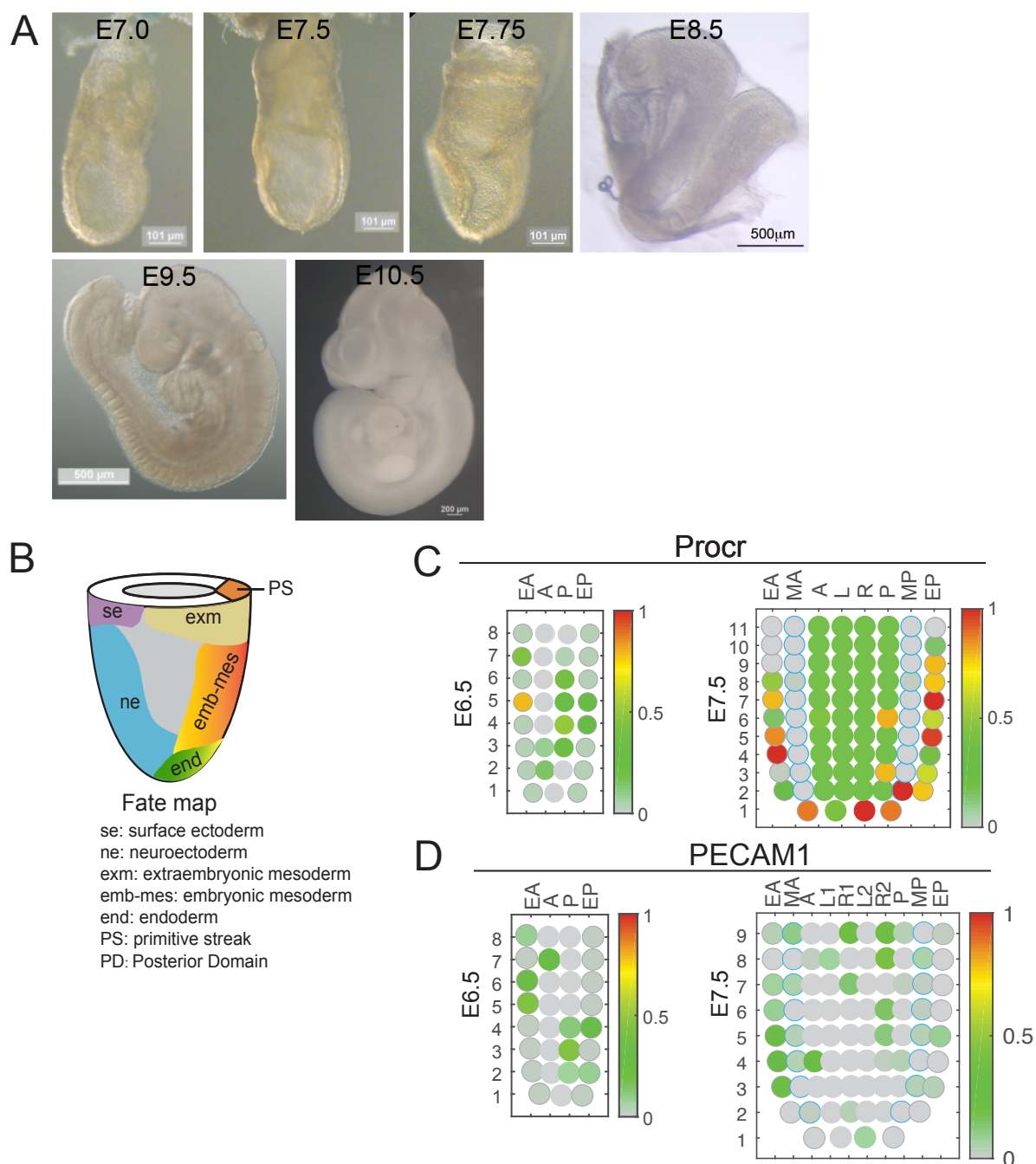


Fig. S2. Expression of Procr during early embryonic development.

(A) X-gal staining of the wild-type embryos. Scale bars as indicated in each image. Embryos from the same pregnant female were harvested and stained simultaneously. Embryos from more than 3 pregnant female mice were analyzed for each time point. **(B)** Illustration of embryonic fate map during gastrulation. **(C-D)** Cornplot showing the spatial expression pattern of Procr and PECAM1(CD31) within E6.5 and E7.5 embryos. EA: anterior endoderm; MA: anterior mesoderm; A: anterior; L: left lateral; R: right lateral; P: posterior; MP: posterior mesoderm; EP: posterior endoderm.

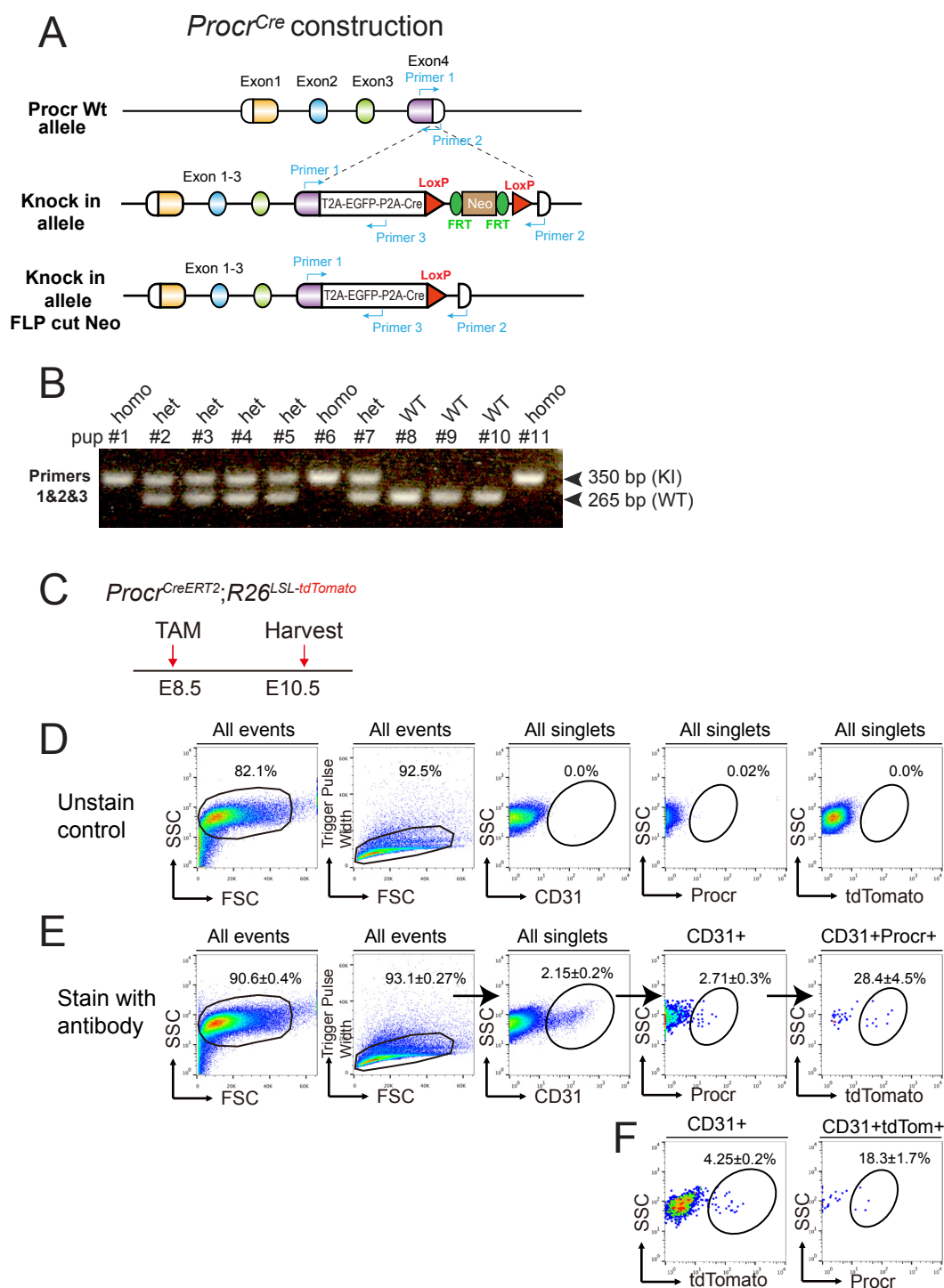


Fig. S3. Generation of the *Procr*^{Cre} knock-in mouse.

(A) Targeting strategy to generate the *Procr*^{Cre} knock-in (KI) mouse. Designs of the genotyping primers are as indicated. (B) Genotyping PCR indicating the positive allele carrying a 350bp band. Mating between two heterozygous parents resulted in proper distribution of wild type, heterozygotes and homozygotes as Mendel's law of segregation. (C) Induction strategy of *Procr*^{CreERT2}; *R26*^{LSL-tdTomato} mouse. (D-F) FACS analyses on *Procr*^{CreERT2}; *R26*^{LSL-tdTomato} embryos after 2 days induction reflecting the labeling efficiency (D) and progeny generation (F). C-F; data from more than 5 embryos were collected.

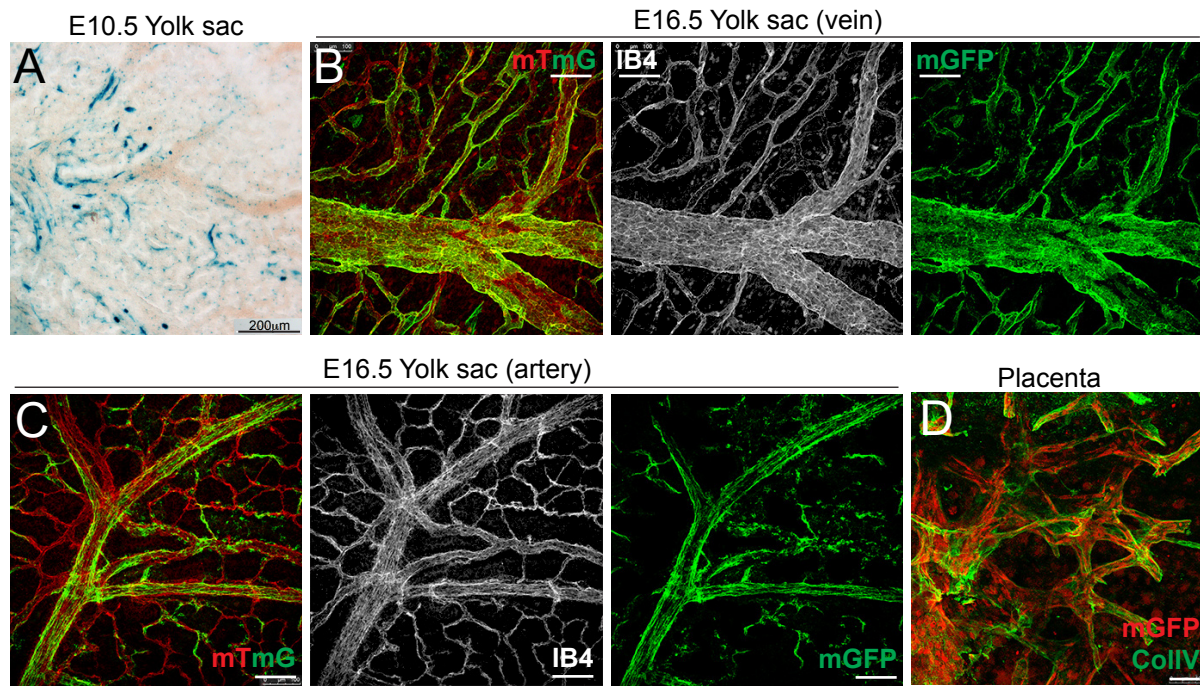


Fig. S4. Procr⁺ cells contribute to yolk sac and placental vasculature.

(A) Representative image of X-gal staining on E10.5 *Procr^{mGFP-2A-LacZ}* shows Procr⁺ cells on yolk sac vessels. Scale bar, 200 μ m. More than 5 embryos were examined. **(B-C)** At E16.5, yolk sac vessels of *Procr^{Cre};R26^{mTmG}* embryo, both veins **(B)** and arteries **(C)** were heavily decorated with mGFP signals, suggesting that they were derived from initially labeled Procr⁺ cells. Isolectin B4 (IB4, identifies endothelial lining) was used to label endothelial layer of vessels. **(D)** Procr⁺ cells also gave rise to the endothelial lining of labyrinth vessels inside the placenta. CollIV, Collagen IV. Scale bars, 50 μ m. More than 5 yolk sac and placenta-attached embryos were harvested lineage tracing.

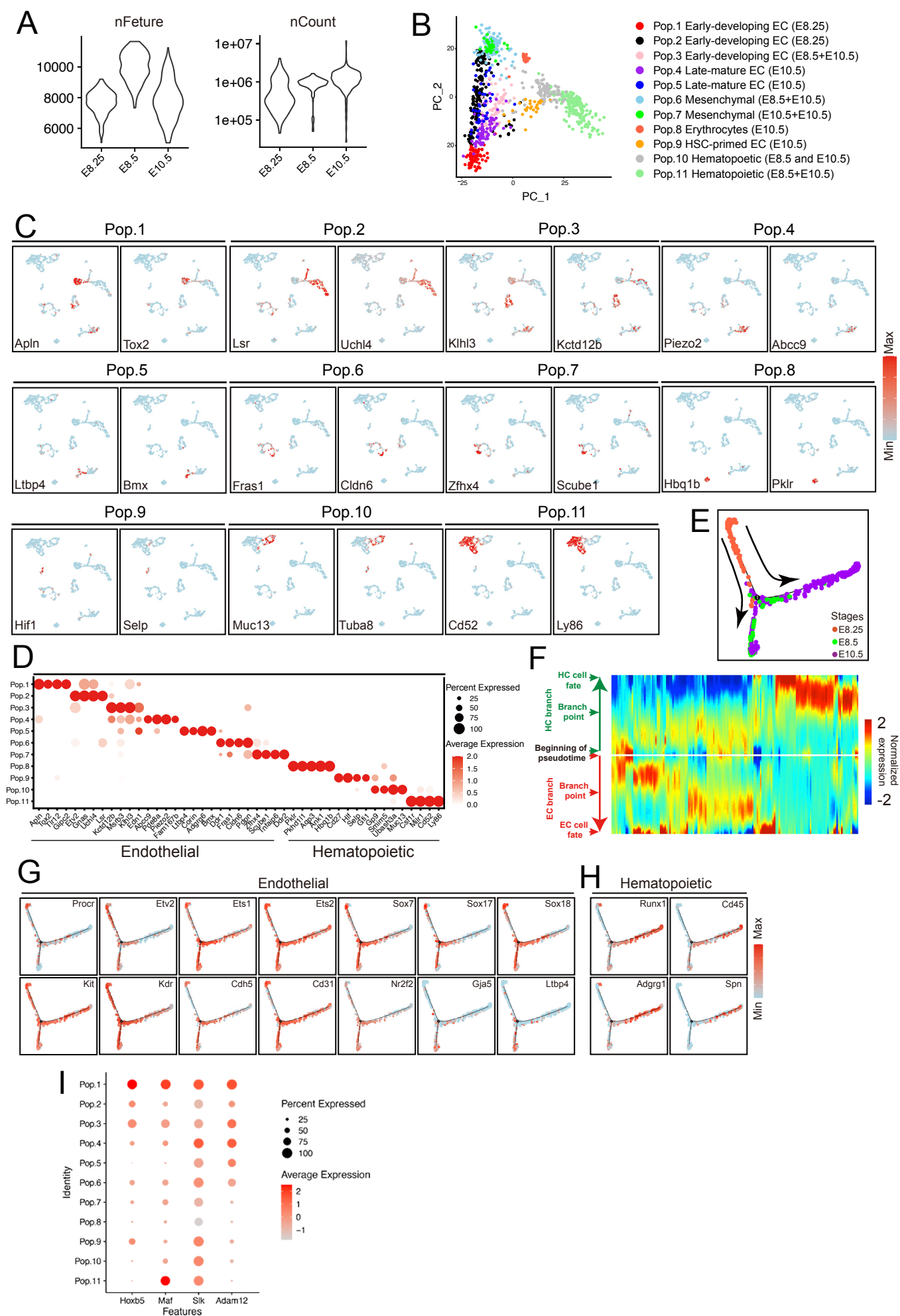


Fig. S5. scRNA-seq reveals Procr+ progenitors give rise to both endothelial and hematopoietic lineage.

(A) Quality metrics for the scRNA-seq data. Distributions of the number of genes detected per cell

(left) and the number of counts per cell (right) are shown. **(B)** PCA analyses of all cells from

E8.25, E8.5 and E10.5 batches. **(C)** Individual gene UMAP plots showing the expression levels and distribu-

tion of representative marker genes of each cluster. The colors ranging from blue to red indicate low to high relative gene expression levels. **(D)** Dot plot for signature genes of

each cluster. The shadings denote average expression levels and the sizes of dots denote

fractional expression. **(E)** Develop-mental trajectory of cells produced by Monocle 2. The colors

denote cell stage. **(F)** The gene branched heatmap depicting the expression of genes along

each branch in pseudotime. An indepen-dent expression pattern is calculated across the entire

pseudotime trajectory for each branch. There-fore, the portion of the trajectory before the

branch point is displayed for each branch separately. Genes are clustered based on expression

pattern across pseudotime. **(G-H)** Individual gene expres-sion on pseudotime trajectory of

known endothelial **(G)** and hematopoietic **(H)** cell types. The colors ranging from blue to red

indicate low to high relative gene expression levels. **(I)** Dot plot for expres-sion pattern of

Hoxb5, *Maf*, *Slk* and *Adam12* in different clusters. The shadings denote average expression

levels and the sizes of dots denote fractional expression.

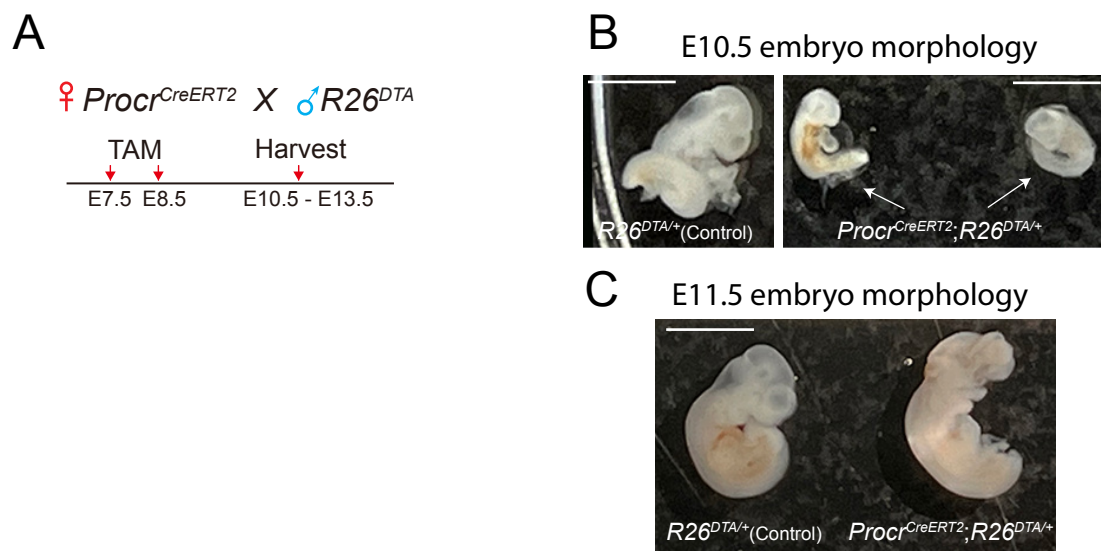
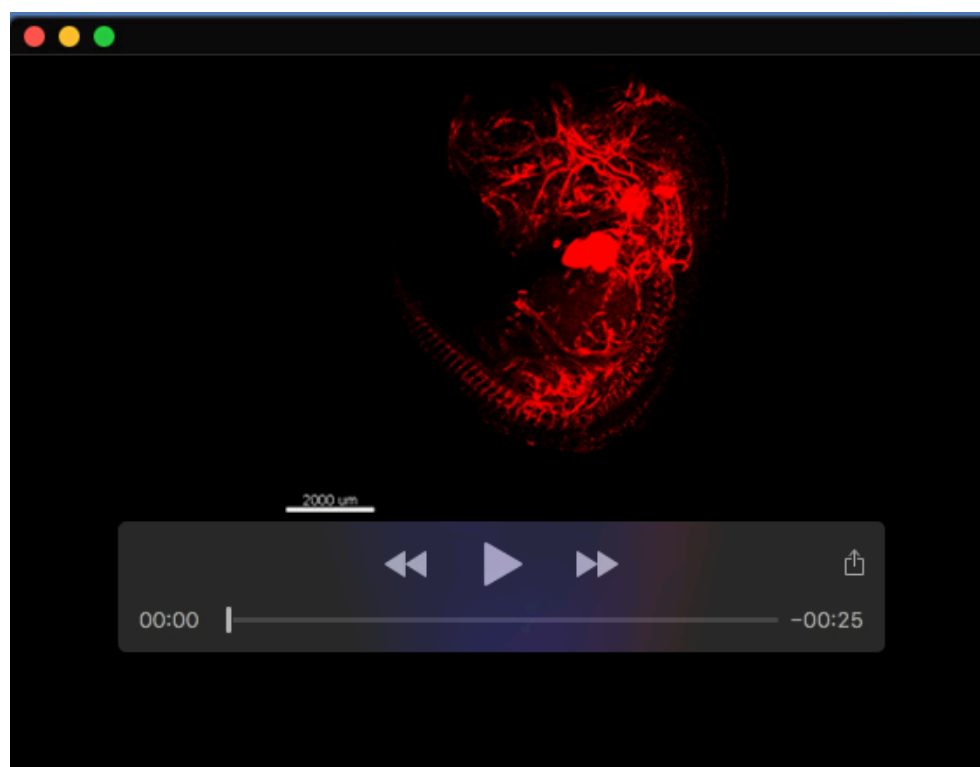


Fig. S6. Ablation of *Procr*⁺ cells cause embryonic lethality.

(A) Schematic illustration of *Procr*⁺ cell ablation strategy. Tamoxifen (TAM) was administered on E7.5 and E8.5 through maternal peritoneal injection, and the uterus was dissected for embryo morphology analysis. **(B-C)** Representative images of the dissected embryos from E10.5 **(B)** and E11.5 **(C)**. Scale bars, 500 μ m. Targeted ablation experiments were performed in at least three pregnant female mice for each harvesting time point.



Movie 1. Whole embryo scanning of E12.5 *ProcrCre*;R26LSL-tdTomato.